HYDROTHERMAL SYNTHESIS OF SINGLE-CRYSTAL RUTILE TiO_2 MICROFLOWERS FOR PHOTOCATALYTIC DEGRADATION OF METHYLENE BLUE

Y. SUN[a], Q. LIU[b], L. ZHU[c], Q. W. TAN[a], Y. X. FAN[a], B. S. ZHAO[a], J. GUO[a], Q. Q. KONG[a,*]

[a]*School of Mechanical Engineering, Chengdu University, Chengdu 610106, Sichuan, China*

[b]*College of Materials Science and Chemical Engineering, Harbin Engineering University, Harbin 150001, Heilongjiang, China*

[c]*School of Chemical Engineering, Yunnan Open University, Kunming 650223, Yunnan, China*

TiO_2 microflowers were successfully fabricated by hydrothermal method using Ti powders as titanium source. The crystal structure and morphology of TiO_2 were characterized by X-ray diffraction, scanning electron microscope and transmission electron microscope. The result reveals that synthesized TiO_2 powders are single-crystal rutile phase with exposed (111) top-facets and (110) side-facets. With assistance of hydrochloric acid and hydrogen peroxide, flower-like microstructures composed of TiO_2 nanorods could be obtained, which display excellent photocatalytic activity by degradation of methylene blue under simulated solar irradiation.

(Received December 25, 2018; Accepted February 15, 2019)

Keywords: Rutile TiO_2, Exposed facets, Hydrothermal, Photocatalytic degradation

1. Introduction

Due to the unique properties, TiO_2 has been intensively investigated as an excellent photocatalyst [1-3]. As we know, nanocrystalline TiO_2 exists in the form of anatase, rutile and brookite phase. In general, among three polymorphs, anatase TiO_2 exhibits higher photocatalytic activity owning to the proper crystal structure, good stability at low temperature and low surface energy [4-6]. However, the band gap of anatase TiO_2 is 3.2 eV while rutile TiO_2 is 3.0 eV. As lower band gap is beneficial for more UV absorption capability and rutile is a thermodynamically stable phase, in some cases rutile TiO_2 demonstrates superior photocatalytic activity than anatase TiO_2 [7].

Usually rutile TiO_2 can be transformed from anatase TiO_2 at high calcination temperature [8-9], which leads to agglomeration and growth of the crystalline grain [10]. In this study, pure rutile phase titania has been prepared at low temperature via a facile hydrothermal method. Furthermore, including the crystal structure, morphology, particle size and crystal facet also play important roles on the photocatalytic performance of TiO_2 [11].

The facet, depending on surface atom arrangement and coordination, significantly affects the adsorption of reactant molecules, surface transfer between photoexcited electrons and reactant molecules [12]. However, there are only a few reports on the rutile TiO_2 with exposed (111) top-facets and (110) side-facets. In order to reduce the recombination of photogenerated electron-hole pair and improve the photocatalytic effiency, here we use spherical titanium powders and successfully synthesize single-crystal rutile TiO_2 microflowers with exposed (111) and (110) facets.

* Corresponding author: kongqingquan@cdu.edu.cn

2. Materials and methods

The spherical titanium powders (0.2 g, average particle size of 20 μm, 99.7%) were mixed with 19 ml deionized water, 10 ml hydrochloric acid and 1 ml H_2O_2, and stirred under a magnetic agitator for 30 min. Then the mixture was transferred to the Teflon-lined autoclave (50 ml) and heated at 200 °C for 18 h. After cooling to room temperature, the product was collected by centrifugation and washed repeatedly with deionized water. Finally, TiO_2 powders were dried at 80 °C. To obtain TiO_2 with good crystallinity, the sample was calcined in a muffle furnace at 450 °C for 2 h.

The crystal structure of Ti powder and TiO_2 was characterized by X-ray diffraction (XRD, DX 2700B, Dandong). The surface morphology and microstructure of samples were determined by field-emission scanning electron microscopy (FESEM, Quanta 450, FEI) and high-resolution transmission electron microscope (HRTEM, Tecnai G2 F20, FEI), respectively.

The photocatalytic activity of rutile TiO_2 single crystal is analyzed by the degradation of methylene blue (MB) solution under a 350W Xenon lamp. 0.1 g TiO_2 powders were dispersed in 100 mL MB solution with concentration of 10 mg/L. Before irradiation, the suspension was stirred in the dark to reach the adsorption equilibrium. The concentration of MB was tested by the absorption spectra with UV-Vis spectrophotometer (UV-6100A, Shanghai Metash).

3. Results

Fig. 1 shows the XRD patterns of Ti powders and TiO_2 samples. It is found that there is no other peak in the Ti diffraction pattern, revealing the purity of Ti powders used as raw material in this study. The XRD pattern of TiO_2 powders without calcination exhibits the typical peaks of rutile TiO_2 single crystal at $2\theta = 27.4^\circ$, 36.1°, 39.1°, 41.2°, 44.1°, 54.3° and 56.6°, corresponding to planes of (110), (101), (200), (111), (210), (211) and (220). Meanwhile the peaks of Ti are not observed, which indicates that Ti powders transform to TiO_2 completely after the hydrothermal reaction. With calcination at 450°C, the peak intensity of rutile TiO_2 is obviously increasing. According to Scherrer Formula [13], crystallite size of rutile TiO_2 could be estimated. As expected the grain size 38.3 nm of TiO_2 annealed at 450°C is larger than that of TiO_2 powders without calcination. Based on above result, it can be concluded that heat treatment can improve the crystallinity of TiO_2 with good phase stability and promote the growth of grain size.

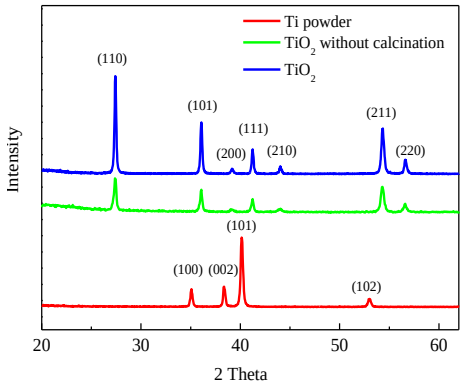

Fig. 1. XRD patterns of Ti source and TiO_2 powders.

Fig. 2 shows SEM images of TiO_2 powders at different magnifications. It is seen clearly that with the combined action of HCl and H_2O_2, TiO_2 of 3D flower structure can be successfully prepared by hydrothermal method at an appropriate temperature and reaction time. According to Fig. 2(d-e), the formation of distinctive flower-like microstructures is observed. Each flower is composed of numerous TiO_2 nanorods with the length of 3 μm. TiO_2 nanorods grow along a certain direction and agglomerate to a flower shape.

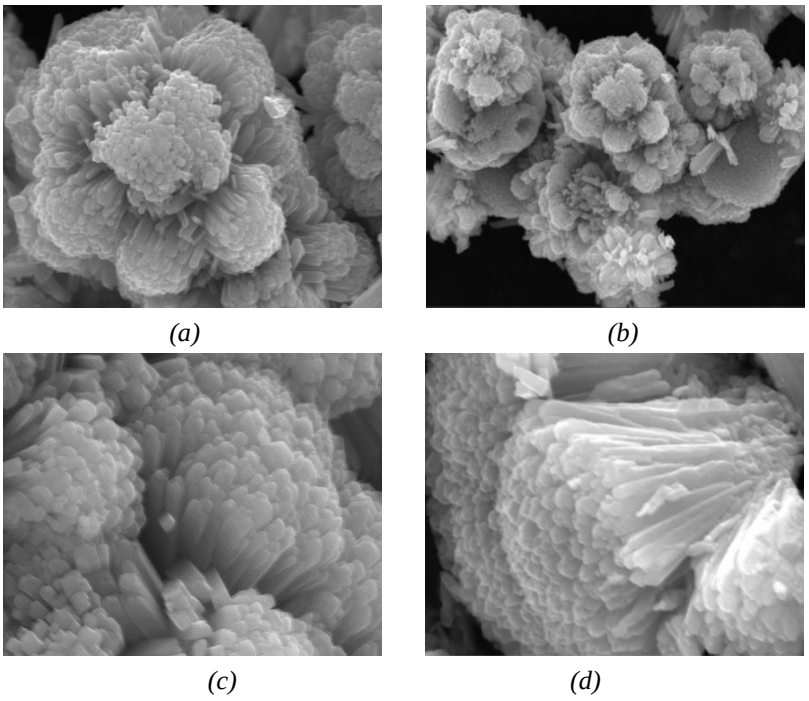

Fig. 2. FESEM images of TiO_2 microflowers at different magnifications.

Further information of TiO_2 microflowers is analysed by HRTEM. The general view of flower-like structure is shown in Fig. 3(a). The diameter of nanorods is detected from the separated nanorods of TiO_2 microflowers. As shown in Fig. 3(c), a diameter of 330 nm is obtained. Fig. 3(d) directly shows a high resolution TEM graphic from the marked area of Fig. 3(c). The measured lattice spacing of 3.3 Å is corresponding to (110) planes of rutile TiO_2. Based on the TEM images, the schematic illustration of TiO_2 with exposed (111) top-facets and (110) side-facets is exhibited in Fig.3 (e). The result reveals the growth mechanism of TiO_2 microflowers under the action of HCl and H_2O_2, which is roughly consistent with the report of [14].

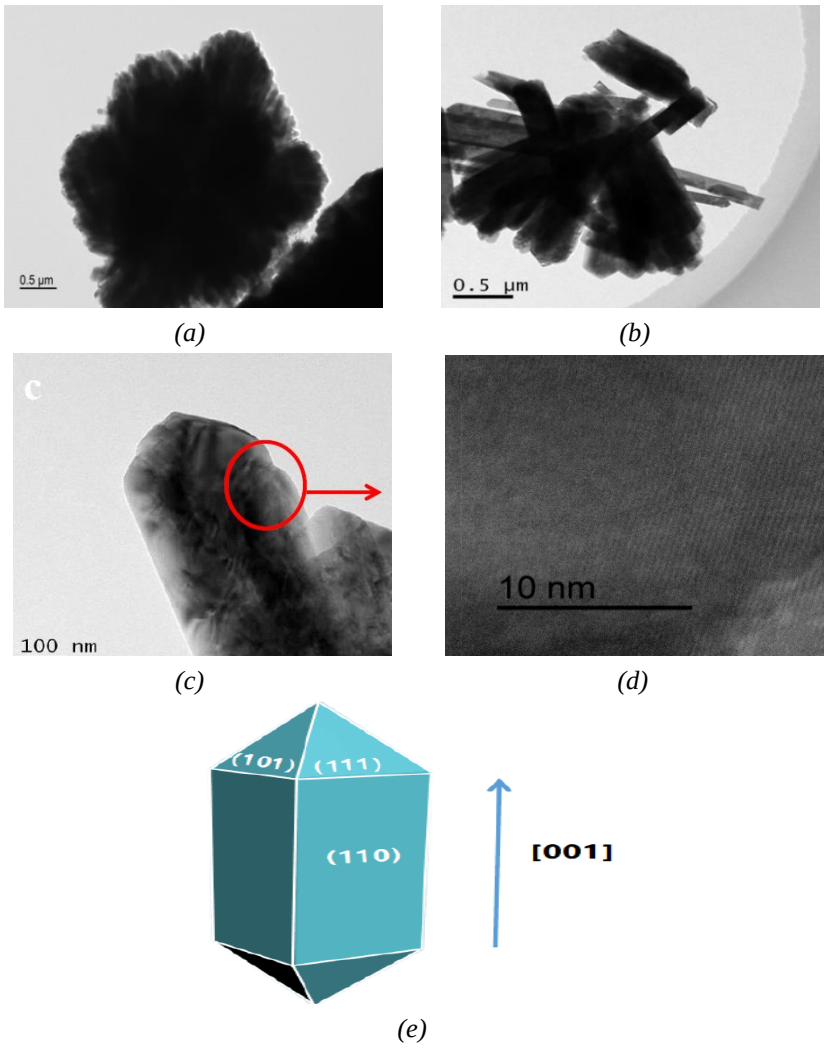

Fig. 3. HRTEM images of TiO_2 microflowers: (a) general view; (b-c) separated nanorods; (d) image of marked area in (c), (e) schematic illustration of rutile single crystal.

Fig. 4 shows the photocatalytic performance of TiO_2 sample under simulated solar irradiation. As shown in Fig. 4 (a), the intensity of the absorption peak at 663 nm decreases dramatically with the irradiation time. When the irradiation time reaches 120 min, there is almost no absorption, which indicates that the degradation of MB dye is nearly completed by the TiO_2 catalyst. Fig. 4(b) is the degradation variation of MB solution during different irradiation times. During the photocatalytic reaction of 60 minutes, the degradation efficiency has reached 80.1%, indicating that the TiO_2 prepared in this study demonstrates superior photocatalytic activity. The decomposition behavior of MB by TiO_2-assisted photocatalytic process can be described by Langmuir-Hinshelwood rate equation. The kinetic fit curve of photocatalytic degradation of MB is shown in Fig. 4 (c), which approximately accords with the first-order kinetics.

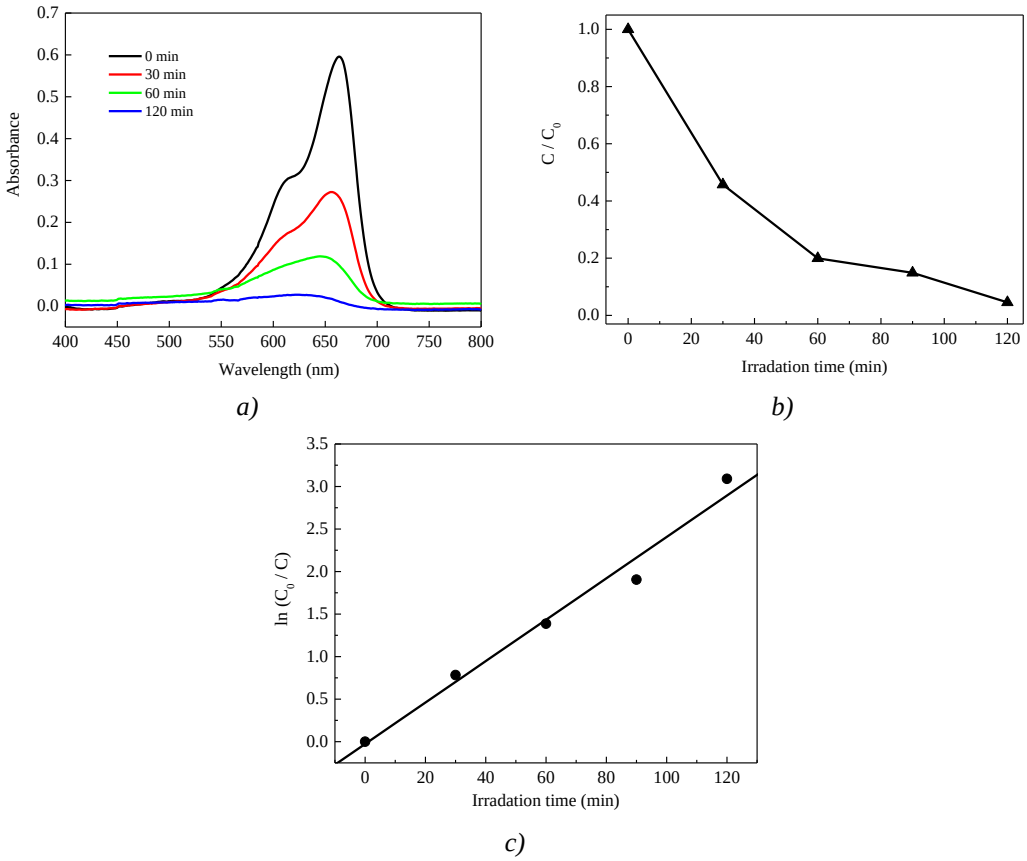

Fig. 4. Photocatalytic activity of TiO_2: (a) UV-vis absorption spectra of MB solution; (b) photocatalytic degradation of MB under solar light; (c) kinetic fit for photocatalytic degradation of MB.

4. Conclusions

Single-crystal rutile TiO_2 microflowers have been successfully prepared by hydrothermal method with combined action of HCl and H_2O_2. The flower shape structure results from the agglomerate of numerous TiO_2 nanorods with the length of 3μm. The TiO_2 microflowers demonstrate superior photocatalytic activity by degradation of methylene blue under simulated solar irradiation. After irradiation of 120 minutes, MB solution is nearly degraded completely.

Acknowledgments

This work is supported by the National Natural Science Foundation of China (No. 51702027).

References

[1] Z. H. Song, H. Zhou, P. Tao, B. Y. Wang, J. Mei, H. Wang, S. G. Wen, Z. C. Song, G. J. Fang, Materials Letters **180**, 179 (2016).
[2] N. Salehifar, A. Nikfarjam, Materials Letters **188**, 59 (2017).
[3] M. Z. Ge, C. Y. Cao, J. Y. Huang, S. H. Li, Z. Chen, K. Q. Zhang, Journal of Materials Chemistry A **4**(18**)**, 6772 (2016).

[4] N. Yuangpho, S. T. T. Le, T. Treerujiraphapong, W. Khanitchaidecha, A. Nakaruk, Physica E: Low-dimensional Systems and Nanostructures **67**, 18 (2015).
[5] T. Luttrell, S. Halpegamage, J. G. Tao, A. Kramer, E. Sutter, M. Batzill, Scientific Reports **4**(2), 4043 (2014).
[6] N. Erdogan, A. Ozturk, J. Park, Ceramics International **42**(5), 5985 (2016).
[7] Y. Wang, L. Z Zhang, K. J. Deng, X. Y. Chen, Z. G. Zou, Journal of Physical Chemistry C **111**(6), 2709 (2007)
[8] J. Yu, B. Wang, Applied Catalysis B: Environmental **94**(3), 295 (2010).
[9] K. L Schulte, P. A DeSario, K. A. Gray, Applied Catalysis B: Environmental **97**(3), 354 (2010).
[10] M. Wu, G. Lin, D. Chen, G. Wang, D. He, S. Feng, R. Xu, Chemistry of Materials **14**(5), 1974 (2002).
[11] J. Chen, H. M Zhang, P. Liu, Y. Wang, X. L. Liu, G. Y. Li, T. C. An, H. J. Zhao, Journal of Colloid and Interface Science **429**, 53(2014).
[12] G. Liu, J. C. Yu, G. Qing (Max) Luc, H. M. Cheng, Chemical Communications **47**(24), 6763 (2011).
[13] V. Uvarov, I. Popov, Materials Characterization **58**(10), 883 (2007).
[14] F. Zuo, K. Bozhilov, R. J. Dillon, L. Wang, P. smith, X. Zhao, C. Bardeen, P. Feng, Angewandte Chemie **124**(5), 6327 (2012).